Data in brief 24 (2019) 103939

Contents lists available at ScienceDirect

Data in brief

journal homepage: www.elsevier.com/locate/dib

Data Article

Data on the negative regulation of invadopodia activity by MLCK

Rachel J. Jerrell [a], Aron Parekh [a, b, c, *]

[a] Department of Otolaryngology, Vanderbilt University Medical Center, US
[b] Vanderbilt-Ingram Cancer Center, Vanderbilt University Medical Center, US
[c] Department of Biomedical Engineering, Vanderbilt University, US

ARTICLE INFO

Article history:
Received 18 March 2019
Received in revised form 10 April 2019
Accepted 15 April 2019
Available online 24 April 2019

Keywords:
Cancer
Invasion
Invadopodia
MLCK
Contractility

ABSTRACT

Actomyosin contractility can promote extracellular matrix (ECM) degradation by invadopodia in cancer cells. However, we previously found that inhibiting myosin light chain kinase (MLCK) with siRNA did not change force generation by the head and neck squamous cell carcinoma (HNSCC) cell line SCC-61. We provide data here that this targeted method of MLCK knockdown (KD) resulted in a significant increase in the amount of ECM degradation, number of actively degrading invadopodia, and the number of total invadopodia formed. These data are related to the research article entitled "Matrix rigidity differentially regulates invadopodia activity through ROCK1 and ROCK2" Jerrell and Parekh, 2016.

1. Data

Actomyosin-generated contractile forces promote ECM degradation by proteolytic subcellular protrusions called invadopodia [1,2]. Cellular contractility can be regulated by several kinases including MLCK; however, we and others have found that MLCK inhibition does not always affect force generation [1,3,4]. Despite this finding in our laboratory using SCC-61 cells, we show here that KD of MLCK increased ECM degradation by SCC-61 cells (Fig. 1A and B) as well as the number of invadopodia

* Corresponding author. Department of Otolaryngology, Vanderbilt University Medical Center, 522 Preston Research Building, 2220 Pierce Avenue, Nashville, TN, 37232, US.
E-mail address: aron.parekh@vumc.org (A. Parekh).

https://doi.org/10.1016/j.dib.2019.103939

Specifications table

Subject area	*cancer research, cell biology*
More specific subject area	*cancer cell invasion*
Type of data	*Table, figure*
How data was acquired	*The invadopodia assay was imaged using a Nikon Ti-E inverted microscope with a Plan Fluor 40× oil immersion objective.*
Data format	*Raw, analyzed*
Experimental factors	*SCC-61 cells were transfected with non-targeted control (NTC) siRNA or siRNA against MLCK.*
Experimental features	*Invadopodia formation and ECM degradation.*
Data source location	*Nashville, TN, USA, Vanderbilt University Medical Center*
Data accessibility	*Data are available in this article.*
Related research article	*R. J. Jerrell, A. Parekh. Matrix rigidity differentially regulates invadopodia activity through ROCK1 and ROCK2, Biomaterials, 84, 2016, 119–129* [1].

Value of the data

- The data presented here reveal the impact of siRNA targeted inhibition of MLCK on invadopodia activity.
- The data may be of interest to researchers studying cancer biology and mechanisms of invasion including the roles of contractility regulators in cancer cell mechanotransduction.
- The data provide the basis for future studies to uncover other mechanisms of MLCK activity in invasive cancer cells.

actively degrading ECM (i.e., colocalized with ECM degradation; Fig. 1Aand C) and the total number of invadopodia (i.e., actively degrading and non-degrading or not colocalized with ECM degradation; Fig. 1Aand D) when compared to NTC in the rigid PAA invadopodia assay which approximates high grade tumor rigidity (raw data presented in Table 1). Western blot data confirming MLCK KD in SCC-61 cells used in these experiments was previously reported and technically described [1].

2. Experimental design, materials, and methods

2.1. Cell culture and MLCK inhibition

SCC-61 cells were cultured as previously described as well as KD of MLCK with siGENOME SMARTpool siRNA (ThermoScientific) or the NTC following the manufacturer's protocol to maximize inhibition while minimizing off-target effects [1].

2.2. Rigid PAA invadopodia assay

Rigid PAAs were synthesized and cast on activated coverslips of 35 mm MatTek dishes as previously described [1]. Briefly, these substrates were composed of a 12%/0.6% ratio of acrylamide/BIS-acrylamide, 0.1% N-hydroxysuccinimide ester, and 230 μg/ml of fibronectin yielding an elastic modulus of 22,692 Pa which mimics tumor rigidity and maximizes invadopodia activity. To detect and evaluate ECM degradation, the rigid PAAs were overlaid with 1% gelatin (crosslinked with glutaraldehyde) and FITC-labeled fibronectin.

2.3. Immunofluorescence

Cells were incubated overnight in invadopodia medium and immunostained in the rigid invadopodia assays as previously described [1]. Briefly, the invadopodia markers actin and cortactin were

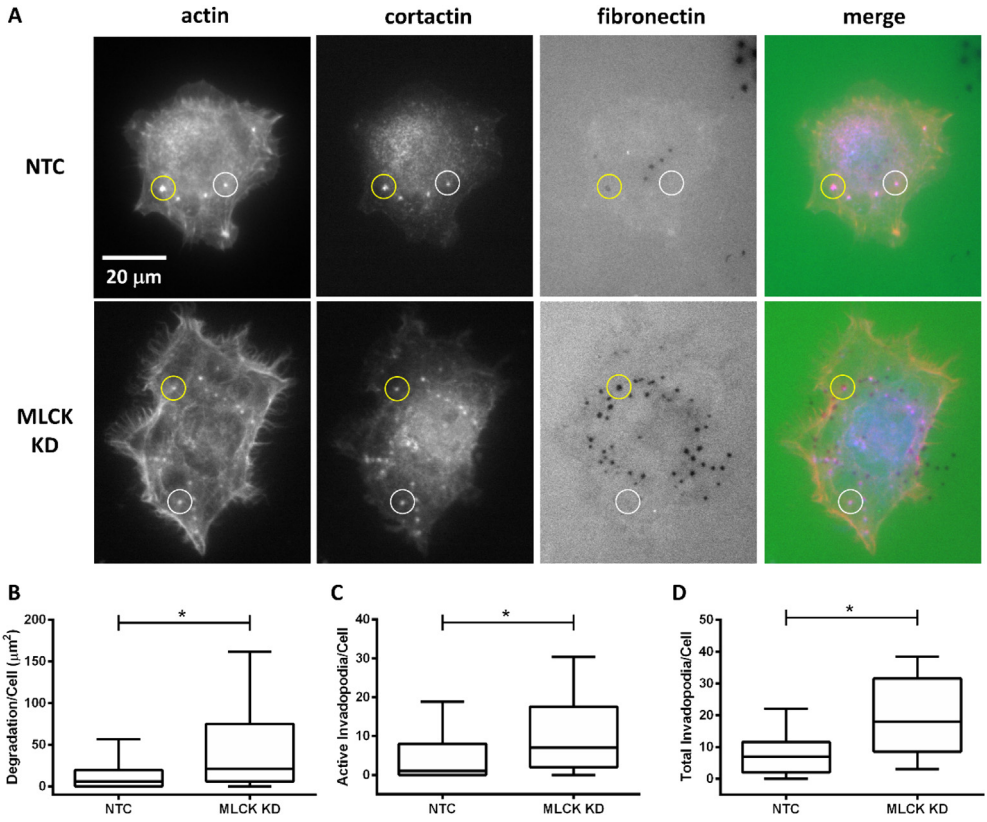

Fig. 1. MLCK negatively regulates invadopodia activity. (A) Representative wide-field fluorescence images of NTC and MLCK KD SCC-61 cells in the rigid PAA invadopodia assay in which invadopodia were identified by the colocalization (pink) of actin (red) and cortactin (blue). Actively degrading (active; yellow circles) invadopodia were identified based on the colocalization of these markers with ECM degradation (i.e., black areas lacking FITC signal). Total invadopodia included the active and non-degrading (white circles) invadopodia. Quantitation of the (B) degradation area per cell, (C) active invadopodia per cell, and (D) total invadopodia per cell for NTC versus MLCK KD. Data are presented as box and whisker plots with the black lines indicating the medians, the whiskers representing the 10th and 90th percentiles, and * indicating $p < 0.05$ for $n = 86–97$ cells for each condition from 3 independent experiments. Scale bar represents 20 μm.

identified with Alexa Fluor 546 phalloidin (Life Technologies) and a mouse monoclonal antibody (EMD Millipore), respectively. Fluorescent images were captured on a Nikon Eclipse Ti-E inverted microscope with a 40× Plan Fluor oil immersion lens. Metamorph software (Molecular Devices) was used for image analyses which included thresholding for ECM degradation and manual quantitation of invadopodia.

2.4. Statistics

Statistical analyses were performed on pooled data using SPSS Statistics (IBM) as previously described [1]. Briefly, data did not pass the normality test and were therefore analyzed with a Mann-Whitney test for comparisons between datasets.

Table 1
Raw data from the immunofluorescence image analyses of NTC and MLCK KD SCC-61 cells in the rigid PAA invadopodia assay.

Experiment	Condition	Replicate	Degradation (μm^2)	Degrading Invadopodia	Total Invadopodia
1	NTC	1	12.7,151,411	7	7
1	NTC	1	6.822,162,246	9	9
1	NTC	1	8.460,459,273	4	4
1	NTC	1	0	0	0
1	NTC	1	0	0	1
1	NTC	1	59.14,985,833	9	10
1	NTC	1	62.18,193,044	14	16
1	NTC	1	0	0	1
1	NTC	1	0	0	0
1	NTC	1	0	0	1
1	NTC	1	0	0	0
1	NTC	1	4.010,159,887	1	1
1	NTC	2	0	0	4
1	NTC	2	0	0	1
1	NTC	2	25.8,948,739	23	23
1	NTC	2	12.00602,747	5	6
1	NTC	2	0	0	2
1	NTC	2	0	0	3
1	NTC	2	1.051,444,361	2	2
1	NTC	2	17.01,872,732	3	3
1	NTC	2	9.316,286,078	7	7
1	NTC	2	0.537,948	0	0
1	NTC	2	0	0	2
1	NTC	2	22.3,982,101	10	10
1	NTC	2	29.02,475,479	4	4
1	NTC	2	18.70,592,874	14	14
1	NTC	2	8.680,529,023	1	4
1	NTC	2	0	0	0
1	NTC	2	19.21,942,482	9	12
1	NTC	2	4.156,873,053	0	7
1	NTC	2	0	0	6
1	NTC	2	0	0	7
1	NTC	2	0	0	1
1	NTC	2	34.6,976,639	10	14
2	NTC	1	7.091,136,385	0	10
2	NTC	1	79.39,627,532	28	38
2	NTC	1	7.94,696,319	2	4
2	NTC	1	0	0	7
2	NTC	1	45.18,765,531	23	26
2	NTC	1	3.521,115,998	1	4
2	NTC	1	59.17,431,052	25	25
2	NTC	1	12.61,733,233	3	8
2	NTC	1	29.416	8	17
2	NTC	1	4.08,351,647	7	8
2	NTC	1	1.66,275	1	7
2	NTC	1	207.6,235,829	32	42
2	NTC	1	31.81,230,496	34	34
2	NTC	1	27.70,433,418	8	10
2	NTC	1	0	0	14
2	NTC	1	55.60,429,014	43	43
2	NTC	1	12.22,609,722	16	22
2	NTC	1	0	0	8
2	NTC	2	10.88,122,652	8	8
2	NTC	2	45.87,231,675	8	22
2	NTC	2	31.83,675,715	8	14
2	NTC	2	120.6,960,317	32	35
2	NTC	2	3.741,185,748	5	7
2	NTC	2	5.159,413,025	0	12
2	NTC	2	10.8,079	5	7

Table 1 (*continued*)

Experiment	Condition	Replicate	Degradation (μm^2)	Degrading Invadopodia	Total Invadopodia
2	NTC	2	0	0	9
2	NTC	2	16.82,310,977	6	7
2	NTC	2	21.24,895,696	7	8
2	NTC	2	65.8,742,118	4	5
2	NTC	2	13.27,754,158	0	0
2	NTC	2	13.54,651,572	0	8
2	NTC	2	15.23,371,713	8	14
2	NTC	2	75.2,394	17	18
2	NTC	2	21.90,916,621	12	18
3	NTC	1	15.25,816,933	8	12
3	NTC	1	0	0	3
3	NTC	1	2.860,906,749	1	4
3	NTC	1	0	0	4
3	NTC	1	0	0	5
3	NTC	1	0	0	0
3	NTC	1	0	0	0
3	NTC	1	0	0	0
3	NTC	1	0	0	5
3	NTC	1	0	0	0
3	NTC	1	0	0	7
3	NTC	1	0	0	0
3	NTC	1	12.51,952,355	10	11
3	NTC	1	0	0	0
3	NTC	1	0	0	2
3	NTC	1	0	0	2
3	NTC	1	8.436,007,079	1	5
3	NTC	1	0	0	1
1	MLCK KD	1	24.40,329,004	16	15
1	MLCK KD	1	20.07,525,163	9	7
1	MLCK KD	1	0	2	0
1	MLCK KD	1	6.308,666,163	5	3
1	MLCK KD	1	28.29,118,896	36	26
1	MLCK KD	1	7.65,354	3	3
1	MLCK KD	1	0	5	0
1	MLCK KD	1	21.00443,502	5	4
1	MLCK KD	1	3.570,020,387	0	0
1	MLCK KD	1	62.01,076,508	19	19
1	MLCK KD	1	0	9	0
1	MLCK KD	1	0	3	0
1	MLCK KD	1	24.94,123,832	14	13
1	MLCK KD	1	16.9,698	3	3
1	MLCK KD	1	9.31,629	7	7
1	MLCK KD	1	0	2	0
1	MLCK KD	1	0	1	0
1	MLCK KD	1	10.61,225,238	15	12
1	MLCK KD	1	111.6,487,198	16	16
1	MLCK KD	1	47.8,529,445	17	12
1	MLCK KD	1	86.78,083,804	9	9
1	MLCK KD	2	4.52,365,597	12	5
1	MLCK KD	2	50.90,946,881	30	30
1	MLCK KD	2	46.19,019,528	10	10
1	MLCK KD	2	25.1,857,568	9	8
1	MLCK KD	2	24.01,204,611	6	6
1	MLCK KD	2	54.4,305,848	22	18
1	MLCK KD	2	85.43,596,734	10	6
1	MLCK KD	2	57.60,937,008	22	22
1	MLCK KD	2	19.21,942,482	5	5
1	MLCK KD	2	13.74,213,327	10	10
1	MLCK KD	2	8.020,319,774	7	6

(*continued on next page*)

Table 1 (*continued*)

Experiment	Condition	Replicate	Degradation (μm^2)	Degrading Invadopodia	Total Invadopodia
1	MLCK KD	2	2.640,836,999	9	0
1	MLCK KD	2	10.07,430,411	4	4
1	MLCK KD	2	11.15,020,066	6	5
1	MLCK KD	2	33.96,409,807	10	6
1	MLCK KD	2	11.90,822,077	8	7
2	MLCK KD	1	161.3,111,267	18	17
2	MLCK KD	1	401.0159,887	47	43
2	MLCK KD	1	72.64,746,966	35	23
2	MLCK KD	1	41.86,215,687	12	7
2	MLCK KD	1	24.1,832	18	5
2	MLCK KD	1	0.684,661,444	32	0
2	MLCK KD	1	93.06,505,201	31	29
2	MLCK KD	1	252.6,404,659	38	38
2	MLCK KD	1	4.03,461	9	8
2	MLCK KD	1	34.35,533,318	22	15
2	MLCK KD	1	93.87,201,628	11	10
2	MLCK KD	1	166.4,216,827	46	40
2	MLCK KD	1	64.18,701,038	33	23
2	MLCK KD	1	263.6,191,082	94	83
2	MLCK KD	1	5.844,074,469	18	2
2	MLCK KD	1	79.7,142	17	7
2	MLCK KD	1	203.5,156,143	40	34
2	MLCK KD	1	11.27,246,163	35	6
2	MLCK KD	1	17.63,003,219	7	5
2	MLCK KD	2	162.411	27	19
2	MLCK KD	2	1.34,487	7	0
2	MLCK KD	2	36.53,157,848	32	12
2	MLCK KD	2	0	33	0
2	MLCK KD	2	94.16,540,076	63	48
2	MLCK KD	2	4.376,942,803	7	0
2	MLCK KD	2	13.8,888	48	2
2	MLCK KD	2	0	18	0
2	MLCK KD	2	0	32	0
2	MLCK KD	2	6.944,423,219	66	3
2	MLCK KD	2	10.24,546,947	32	7
2	MLCK KD	2	190.4,583,442	38	34
2	MLCK KD	2	119.8,891	31	10
2	MLCK KD	2	77.12,222,124	34	27
2	MLCK KD	2	4.35,429	9	2
2	MLCK KD	2	126.8,823,909	38	32
2	MLCK KD	2	44.67,415,923	21	7
2	MLCK KD	2	114.6,104	62	46
2	MLCK KD	2	36.8,006	23	5
2	MLCK KD	2	180.3,349,339	26	22
2	MLCK KD	2	116.0990,192	32	27
2	MLCK KD	2	155.320,339	34	26
2	MLCK KD	2	41.2,508	44	8
3	MLCK KD	1	0	14	0
3	MLCK KD	1	121.0,383,624	28	24
3	MLCK KD	1	12.69,068,891	18	2
3	MLCK KD	1	3.12,988	3	0
3	MLCK KD	1	8.876,141,581	22	4
3	MLCK KD	1	8.411,553,388	24	3
3	MLCK KD	1	0	0	0
3	MLCK KD	1	0	7	0
3	MLCK KD	1	0	10	0
3	MLCK KD	1	19.61,065,993	19	6
3	MLCK KD	1	10.41,663,483	30	6
3	MLCK KD	1	52.49,886,144	21	20
3	MLCK KD	1	5.403,934,969	17	1

Table 1 (*continued*)

Experiment	Condition	Replicate	Degradation (μm^2)	Degrading Invadopodia	Total Invadopodia
3	MLCK KD	1	1625.948,669	0	0
3	MLCK KD	1	41.32,420,742	11	10
3	MLCK KD	1	19.14,606,869	20	17
3	MLCK KD	1	11.12,574,847	26	7
3	MLCK KD	1	37.92,536,432	24	15

Acknowledgments

Research reported in this publication was previously supported by the National Institutes of Health grant K25CA143412 from the National Cancer Institute to A.P. Additional support was provided at the time by the Vanderbilt Clinical and Translational Science Award UL1TR000445 from the National Center for Advancing Translational Sciences and resources from the Vanderbilt Advanced Computing Center for Research and Education. The content is solely the responsibility of the authors and does not necessarily represent the official views of the National Institutes of Health or National Center for Advancing Translational Sciences. Current support was provided by the Research Scholar Grant RSG-15-226-01-CSM from the American Cancer Society to A.P.

Transparency document

Transparency document associated with this article can be found in the online version at https://doi.org/10.1016/j.dib.2019.103939.

References

[1] R.J. Jerrell, A. Parekh, Matrix rigidity differentially regulates invadopodia activity through ROCK1 and ROCK2, Biomaterials 84 (2016) 119–129.
[2] R.J. Jerrell, A. Parekh, Cellular traction stresses mediate extracellular matrix degradation by invadopodia, Acta. Biomater. 10 (5) (2014) 1886–1896.
[3] K.A. Beningo, K. Hamao, M. Dembo, Y.L. Wang, H. Hosoya, Traction forces of fibroblasts are regulated by the Rho-dependent kinase but not by the myosin light chain kinase, Arch. Biochem. Biophys. 456 (2) (2006) 224–231.
[4] M.A. Wozniak, R. Desai, P.A. Solski, C.J. Der, P.J. Keely, ROCK-generated contractility regulates breast epithelial cell differentiation in response to the physical properties of a three-dimensional collagen matrix, J. Cell Biol. 163 (3) (2003) 583–595.